CSIRO PUBLISHING

International Journal of Wildland Fire **2012**, *21*, 583–590
http://dx.doi.org/10.1071/WF11018

Application of QuickBird imagery in fuel load estimation in the Daxinganling region, China

Sen Jin[A,C] *and Shyh-Chin Chen*[B]

[A]College of Forestry, Northeast Forestry University, Harbin, Heilongjiang Province, 150040, PR China.
[B]Pacific Southwest Research Station, USDA Forest Service, Riverside, CA 92507, USA.
[C]Corresponding author. Email: jins-cf@nefu.edu.cn

Abstract. A high spatial resolution QuickBird satellite image and a low spatial but high spectral resolution Landsat Thermatic Mapper image were used to linearly regress fuel loads of 70 plots with size 30 × 30 m over the Daxinganling region of north-east China. The results were compared with loads from field surveys and from regression estimations by surveyed stand characteristics. The results show that fuel loads were related to stand characteristics, such as stand mean diameter at breast height and stand height. As the QuickBird image using the shadow fraction method represented the stand characteristics well, fuel loads were well estimated from the QuickBird image. QuickBird estimations outperformed those from the lower spatial resolution Thermatic Mapper image. For many fuel classes, the QuickBird estimations were as good as those regressed from surveyed stand characteristics, and thus similar to the surveyed fine and total dead fuel loads. However, coarse fuel loads were not estimated as well using both satellite images owing to their intrinsic low association with stand characteristics. Despite this limitation in estimating coarse fuels, very-high-resolution images such as QuickBird are still valuable in estimating fine fuels, which are critically important in the practice of fire management.

Additional keywords: remote sensing, shadow fraction.

Received 31 January 2011, accepted 14 November 2011, published online 25 May 2012

Introduction

Spatial information on forest fuel loads is crucial to forest fire management. Ground surveying methods such as fixed-area plots, planar intersect and photo loads (Sikkink and Keane 2008) are the most accurate methods for estimating fuel loads, but are quite labour-intensive for large-scale areas. Therefore, remote sensing data have been widely used for fuel information extraction, which can provide spatially continuous fuel information. This is a promising method owing to low cost and better information accessibility. However, most studies have focussed on forest fuel classification (Oswald *et al.* 1999; Keane *et al.* 2000; Keane *et al.* 2001; Banninger *et al.* 2002; Giakoumakis *et al.* 2002; Riaño and Chuvieco 2002; Miller *et al.* 2003; Andersen *et al.* 2005; Arroyo *et al.* 2006; Jia *et al.* 2006; Mitri and Gitas 2006; Lasaponara and Lanorte 2007; Mutlu *et al.* 2008), whereas relatively few studies have been conducted to estimate fuel load (Scott *et al.* 2002; Brandis and Jacobson 2003; Reich *et al.* 2004; Skowronski *et al.* 2007; Wang and Jin 2008). Consequently, improving fuel load estimations from remote sensing data remains a great challenge.

Current remote sensing methods to estimate fuel loads can be grouped into two categories: spectral reflectance-based (SRB) and stand characteristics-based (SCB) methods. SRB methods directly regress fuel loads from independent variables of image band values and other auxiliary variables such as topography (Reich *et al.* 2004; Wang and Jin 2008). Reich *et al.* (2004) established fuel-loading linear prediction equations using Landsat Thermatic Mapper (TM) band data, slope, aspect and forest classes as predictive variables for forest in the Black Hills, South Dakota, USA. Wang and Jin (2008) established non-linear fuel-loading prediction equations using TM data and topographic variables by ridge regression for forest in Maoershan Mountain in Heilongjiang Province, China. These are direct SRB methods.

SCB methods, however, retrieve stand characteristics first by means of vegetation indices computed from remote sensing data, then estimate fuel loads from these derived stand characteristics empirically (Scott *et al.* 2002; Brandis and Jacobson 2003; Skowronski *et al.* 2007). Scott *et al.* (2002) first estimated crown cover percentages from aerial photos, then estimated total fuel loads by established linear prediction equations for three vegetation types in the Jemez Mountains of northern New Mexico, USA. Brandis and Jacobson (2003) used two distinct SCB methods to estimate fuel loads from TM data in New South Wales, Australia. Their first method obtained vegetation types from a classification map produced from TM data and then used existing vegetation-specific fuel-load prediction equations by Olson (1963) to estimate the fuel loads. Their second method first estimated woody biomass weights from a vegetation index composed of the pixel ratio of the near infrared band to the red band, tree height obtained from a classified vegetation map, and descriptive data from a field survey. Canopy biomass of leaf and twigs was then deduced from the woody biomass weights

Journal compilation © IAWF 2012

via allometric relationships. Finally, the litter accumulation was computed from relationships derived from the canopy biomass of leaf and twigs and decomposition rate. Skowronski *et al.* (2007) used LIDAR (Light Detection and Ranging) data to estimate canopy height as the first step and then estimated total fuel load from the canopy height through an existing relationship.

The accuracy of a SRB method depends on empirical correlations between fuel loads and derived spectral indices from remote sensing data. The success of a SCB method relies on the quality of two empirically derived relationships. One is that of the fuel load to stand characteristics, which is determined by the complexity of the stands studied (Keane *et al.* 2000). The other is remotely sensed data to stand characteristics. The robustness of all these empirical relationships, and hence the accuracy of the methods, varies among indices deduced from remote sensing images and fuel classes.

Spatial resolution of remote sensing images affects the indices used for fuel-load estimation. Thirty metres was the highest spatial resolution of remote sensing images previously used for fuel load estimation except in LIDAR data. A pixel in the image represents a 30×30-m area in the field. This approximately equals the size of the plot usually used for fuel-load ground surveys. Therefore, indices can be deduced from band values of only one pixel (hereafter referred to as a 'one-pixel index'). Consequently, the band values are a mixture of the reflectance of different ground objects, such as trees, shrubs, grasses and others objects within the plot. As such, it is very difficult to distinguish spatial information of stand structure from these one-pixel indices.

The spatial resolution of very-high-resolution images (VHRIs) is usually less than 5 m, for example, 2.41 and 0.61 m for QuickBird. Therefore, there are many pixels in the image corresponding to a 30×30-m plot in the field ($\sim$2500 pixels for a QuickBird panchromatic image), and indices deduced from VHRIs for such plots are a combination of band values of many pixels (hereafter referred to as multipixel indices). They contain more spatial information of stand structure than one-pixel indices can provide. Stand characteristics, such as stand mean diameter at breast height (DBH) and mean tree height, can be accurately derived from these multipixel indices (Kayitakire *et al.* 2006; Leboeuf *et al.* 2007). But VHRIs have not been used for fuel load estimation.

One method of classifying forest fuels follows the USDA Forest Service method (Deeming *et al.* 1972) where there are litter, 1-h (1-h time-lag), 10-h, 100-h and 1000-h fuels (Deeming *et al.* 1972), plus total dead fuel and total fuel. The branch and twig diameters of 1-h fuel are less than 0.63 cm, 10-h fuel are between 0.63 and 2.54 cm, 100-h fuel are between 2.55 and 7.62 cm, and 1000-h fuel are greater than 7.62 cm. Litter, 1-h and 10-h fuels are fire starters and are also called fine fuels in fire danger rating systems. All these time-lagged fuels are collectively named total dead fuel. Total fuel includes dead and live fuels and is also very important in fire behaviour simulation, especially for energy release computation. This fuel classification system has been introduced and widely used in China (Hu 2005; Hu and Wang 2005; Wang and Jin 2008).

Among these fuel classes, the total fuel load equals the surface biomass and can be well estimated from one-pixel indices (Zhao 2001; Zhao and Li 2001). However, other fuels, such as fine fuels, are located below the canopy layer and their loads are determined by two distinct factors: the annual production and decomposition rates of the fuels (Brandis and Jacobson 2003). These two factors are closely associated with stand characteristics (Liu *et al.* 1995; Hu 2005; Hu and Wang 2005, Shan *et al.* 2005). Therefore, these fuel types are not directly detectable from remote-sensed images. The total dead fuel of a stand is also closely related to stand characteristics such as DBH, mean tree height and closure (Liu *et al.* 1995; Scott *et al.* 2002; Hu 2005; Hu and Wang 2005, Shan *et al.* 2005; Mitsopoulos and Dimitrakopoulos 2007). As fine fuel loads are more critical in fire behaviour simulation, they need to be more accurately estimated. Although it has been shown that fine fuel loads can be retrieved from one-pixel indices by either the SRB or SCB methods (Brandis and Jacobson 2003; Reich *et al.* 2004; Wang and Jin 2008), high-resolution multipixel indices should perform even better because they can reflect more stand spatial information, which has a strong relationship to fine fuel loads.

Consequently, it is reasonable to hypothesise that fuel-load estimations, at least fine fuels, can be improved by using multipixel indices from VHRIs over low-resolution one-pixel indices. To examine this hypothesis and to determine the extent of any improvement, a VHRI QuickBird image was used to estimate fuel load in a typical region of north-east China that is affected by frequent severe forest fires. These estimates were compared with those by field survey and by the higher spectral resolution but lower spatial resolution TM image.

Materials and methodology

Study area

The study area is located at the Yanjiang Forest Farm, Tahe Forestry Bureau, Daxinganling Region, Heilongjiang Province, China (Fig. 1). Its central geographical coordinates are 53°08′25.27″N, 124°18′26.00″E. The area is in a cold temperate continental monsoon climate zone, cold and dry in winter and cool in spring and autumn. Summer is short. The annual mean precipitation is 428 mm, concentrated in the summer monsoon wet season. The annual mean temperature is −2.8°C with accumulated temperature within growth season 1068.5°C. The zonal soil is brown forest soil. The elevation is 300–900 m with generally flat topography (Zhou 1991).

The original vegetation is larch (*Larix gemelini*)-dominated boreal forest mixed with birch (*Betula platyphylla*) and poplar (*Poplus dividiana*), occupying 49.67% of the area. *Larix gemelini* is a deciduous coniferous species that can grow on dry or wet sites and is the most fire-resistant species in the region, with increasing bark thickness after fires (Zhou 1991). Scots pine (*Pinus sylvestris* var. *mongolica)*, occupying 4.83% of the area, is an evergreen conifer that grows high on dry slopes and is more combustible than larch owing to dry site conditions. Birch and poplar, occupying 44.99% of the area, occur in burned areas as pioneer species after a severe burn or as accompanying species in other stands. Fire history studies suggest that fire plays a major role in sustaining the larch-dominated ecosystem in the region (Zhou 1991). On average, 43 fires burned annually, with an average burned area of 160 000 ha from 1965 through 2005 in the whole Daxinganling Region of 8 460 000 ha (Zhang 2008).

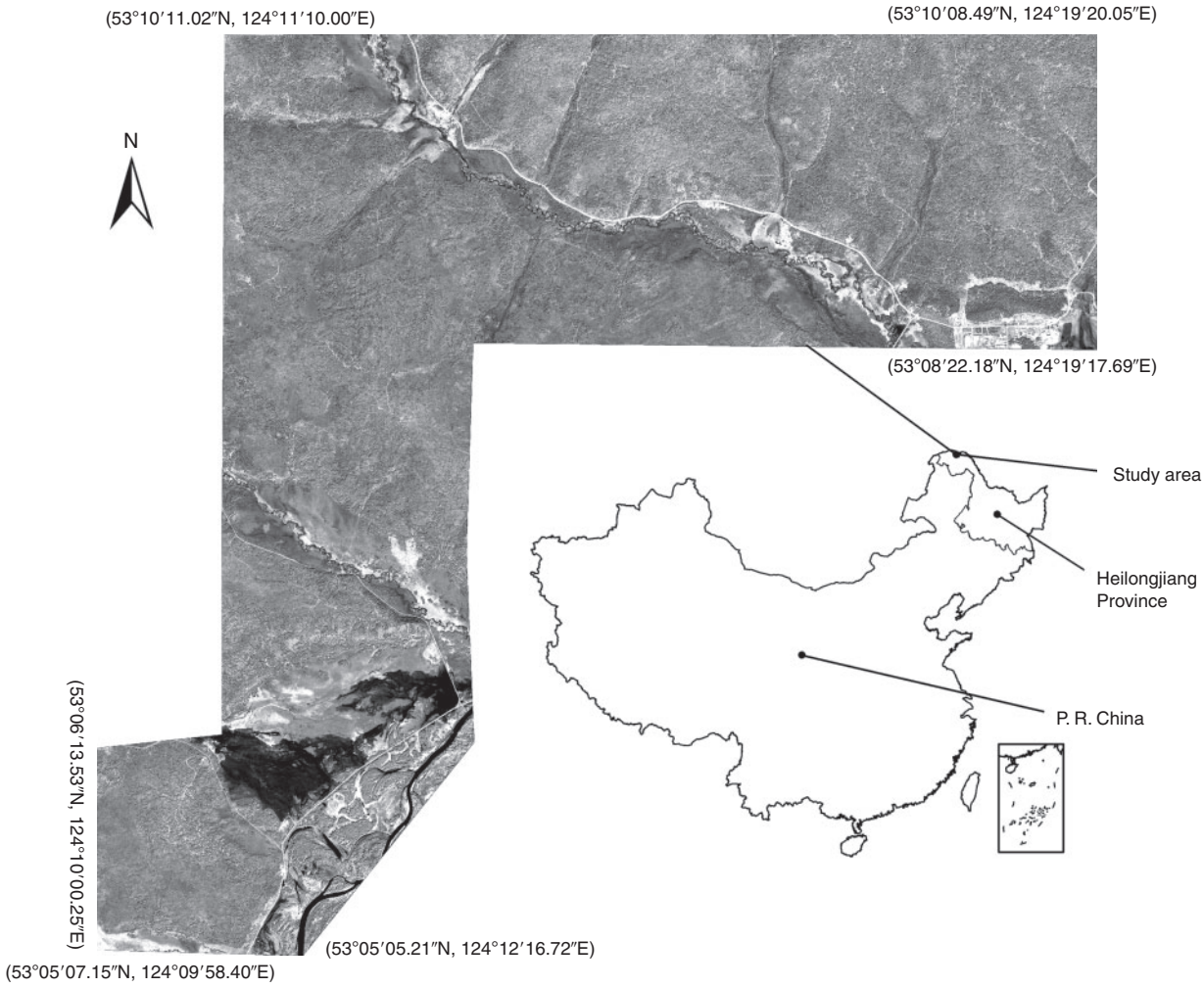

Fig. 1. Location of study area (the map of the study area is from the panchromatic QuickBird image).

Current forests have either regenerated naturally following severe fire or have become secondary forests that followed heavy clear-cutting. Thus the stands are mainly mixed forest with rather low heterogeneity. Fire prevention and suppression activities have significantly reduced fire occurrence and have prolonged the fire return intervals in the region (Jin 2002).

QuickBird and TM images

A geometrically corrected and atmospherically rectified QuickBird image taken at 1036 : 31 hours, 11 April 2006, covering the region using 2.4-m resolution, four bands data and 0.61-m resolution panchromatic data was analysed. The image's solar azimuth and elevation angles are 162.6° and 58.4°. The QuickBird image covered an area of 4600 ha. The data were not orthorectified as the study area is generally flat.

A TM image with six bands (bands 1–5 and band 7) and a resolution of 30 m of the same area was taken at 1436 : 39 hours, 5 July 2006. The image was also geometrically corrected and atmospherically and radiometrically rectified. The image's solar azimuth and elevation angles are 147° and 57°. The atmospheric corrections were made by *ENVI* based on the MODTRAN4+ atmospheric radiative transfer model. The TM image was reprojected from Transverse Mercator to Universal Transverse Mercator projection, and the QuickBird image projection was done with *Imagine 8.6* (Leica Geosystems GIS and Mapping LLC 2003, Leica Geosystems AG, Heerbrugg, Switzerland).

Seasonality does affect fuel estimations from remote sensing data. The QuickBird and TM images used here were acquired 2 months apart. However, when using QuickBird images, April is a better month for shadow fraction (SF, see definition below) estimation than the tree-growing summer months. Summer is a better season for estimating TM indices, which have a better relationship with vegetation growth. Therefore, we expected optimal fuel load estimations from these two images and any discrepancy due to the different acquisition times was expected to be quite limited.

Field survey

In the summer of 2006, 75 forest plots of 30 × 30 m each were set and surveyed. These plots were positioned by a GPS set with 15-m accuracy. To accurately geoposition these plots on the QuickBird image, only plots with measurable distances and directions to identifiable landmarks (such as road intersections) on the QuickBird image were selected. Reich *et al.* (2004) used

151 plots for a study area of more than 80 000 ha and Scott *et al.* (2002) used 116 plots for an area of more than 650 000 ha. Thus, 75 plots were considered sufficiently representative for our relatively small study area. This area posses little vegetation variety. The stands were mainly secondary forests grown after clear-cutting with ages ranging from 40 to 75 years.

The DBH and heights of trees with DBH greater than 5 cm in each plot were tallied by species. A transect interception method (Brown, *et al.* 1982) with transect length of 60 m was used for measuring all time-lagged fuel loads. This method allowed quick measurement of fuel loads with sufficient accuracy. Four quadrats of 0.5×0.5 m in each plot were randomly set and all litter in the quadrats was weighed on site. Samples were taken back to the laboratory and oven-dried at 105°C for 8 h, then weighed again. The fuel moisture contents of the litter were computed and the mean of the litter masses from the four quadrats was taken as the litter load of the plot and prorated to per hectare. Following Feng *et al.* (1999), grass and shrub loads were measured by the subplot method with sizes of 1×1 and 2×2 m. Similarly, living tree loads were computed from allometric equations (Feng *et al.* 1999). All the above dead fuels were summed up as total dead fuel and total fuel load of the plot.

Fuel loads estimations from stand characteristics

Five of the 75 surveyed plots, which consisted of seed orchard or had been recently thinned, were excluded from the dataset because the loads in these plots were significantly altered by human activity. As all plots were in the secondary forest area grown after severe clear-cutting, differences in species composition and structure among the plots were not as great as those in the original forest. Thus, it was assumed that relationships between fuel loads and stand characteristics of plots did not vary with dominant species over these plots. We did, in fact, consider dominant species in the fuel load regression. However, the result (not shown) indicated little effect from species variation. The data were pooled and only one set of fuel load estimation equations was established using the surveyed fuel loads and stand features of the remaining 70 plots by multiple regression. The commonly used equation, hereafter referred to as SC, is:

$$L = b_0 + b_1 H + b_2 D \tag{1}$$

where L is the fuel load (Mg ha^{-1}), D the stand mean DBH (cm), H the stand mean tree height (m), and b_0, b_1 and b_2 are regression coefficients. This equation was also used in Liu *et al.* (1995) and Hu (2005) for the same region.

To test the robustness of the regression, errors were computed 70-fold by cross-validation. Each time, 50 plots were randomly chosen for regression training, and the regression model obtained was subsequently used for estimation and validation on the remaining 20 plots. Then the same procedure was repeated 70 times. Root mean square errors (RMSE) were computed for validation as:

$$\mathrm{RMSE} = \sqrt{\left(\sum_{i=1}^{n} (Y_i - y_i)^2\right)/n}$$

where Y_i and y_i denote the estimated and measured values, and $n = 20$ is the number of validation plots. Twenty plots were used instead of one for each validation to provide enough samples to compute one RMSE. This cross-validation enabled further multiple comparisons and prevented a random noise signal, especially from those measurements weakly or moderately related to fuel loads. If most of the 70 validations have similar relationships, then the relationship is robust and unique. This cross-validation method was applied to all load estimations from stand characteristics and images.

Fuel load estimations from the TM image

For our study, 25 compound indices (Zhang *et al.* 2003) were computed for each plot using band data from the TM image. They are B_1, B_2, B_3, B_4, B_5, B_7, $B_1 - B_2$, B_2/B_1, $B_2/(B_2 + B_1)$, $(B_2 - B_1)/(B_2 + B_1)$, $(B_2/B_1)^{0.5}$, $(0.5 + (B_2 - B_1)/(B_2 + B_1))^{0.5}$, $B_4 - B_3$, $B_4/(B_4 + B_3)$, $B_3/\sum$, B_4/B_3, $(B_4/B_3)^{0.5}$, $(B_4 - B_3)/(B_4 + B_3)$, $(0.5 + (B_4 - B_3))/B_4 + B_3))^{0.5}$, $(B_4 - B_3)/(B_4 + B_3)^{0.5}$, B_7/B_3, B_4B_3/B_7, $(B_5 + B_7 - B_2)/(B_5 + B_7 + B_2)$, $(B_4 + B_5 - B_2)/(B_4 + B_5 + B_2)$, B_4B_5/B_7, where B_i stands for the value of band i, and $\sum$ represents the sum of all band values. Estimation of stand characteristics and biomass from remote sensing data using these indices is similar to our study. The loads of various fuel classes were subsequently estimated using both SRB and SCB methods. This SRB method, hereafter referred to as TM1, estimated the loads directly from the indices using multiple linear equations established by conducting forward stepwise regressions over the surveyed loads and the 25 indices. For the SCB method, stand mean DBH and mean tree height were estimated first from the TM indices using a multiple linear equation established by conducting forward stepwise regressions of the surveyed stand mean DBH or mean tree height with the 25 indices. Then Eqn 1 was used to compute the respective loads using stand characteristics deduced from TM indices. Hereafter, we refer to this method as TM2.

Fuel load estimations from QuickBird imagery

Pixel values of the panchromatic data over each plot were extracted with *Imagine 8.6* from the QuickBird image. Taking advantage of the high spatial resolution, stand characteristics such as stand mean DBH and tree height were then estimated from these panchromatic data by a SF method (Leboeuf *et al.* 2007). Tree shadow (TS) is caused by tree crowns in images. The assumption is that the taller and wider the tree trunk, the larger the tree crown, and hence the higher fraction of TS in a plot. In the panchromatic image, when the darkness of a pixel is higher than a given value called the TS threshold, it is regarded as TS. The area fraction of TS in a plot is called the shadow fraction. Two parameters, scale and TS threshold, should be determined first before applying the method. The scale for SF is the computational unit size, i.e. 30×30 m, which facilitates matching the plot sizes in the field survey to the TM image pixel. The TS thresholds for defining individual TSs were set to the values when the maximum correlation coefficients of SF with surveyed mean DBH and tree height occurred. Presumably the satellite-viewing zenith and azimuth and solar zenith and azimuth angles vary with season and time of day and thus affect SF. However, these variation effects can be eliminated by

Table 1. Statistics of stand characteristics and fuel loads of 70 plots surveyed

	DBH (cm)	Mean tree height (m)	Litter load	1-h fuel load (Mg ha^{-1})	10-h fuel load (Mg ha^{-1})	100-h fuel load (Mg ha^{-1})	1000-h fuel load (Mg ha^{-1})	Total dead fuel load (Mg ha^{-1})	Total fuel load (Mg ha^{-1})
Mean	14.9	11.8	1.852	5.081	6.719	2.583	2.411	18.646	69.101
Median	15.0	11.9	1.937	4.895	6.673	1.410	2.049	19.215	64.921
Standard deviation	2.4	1.6	0.959	2.014	2.152	2.777	2.178	6.369	36.052
Minimum	10.4	8.3	0.156	1.290	2.667	0	0	8.085	17.244
Maximum	20.1	16.2	4.794	10.240	12.667	10.585	7.677	32.332	155.441

normalising SF to common geometry (Leboeuf *et al.* 2007). As the area covered by the QuickBird image is only 4600 ha, these effects were assumed to be quite limited, so SF was not normalised here.

Fuel loads were estimated by two methods. For the SRB method (QB1 hereafter), the loads were estimated directly from SF using linear regression equations. For the SCB method, stand mean DBH and H were first estimated by linear equations established between field-surveyed DBH, H and SF computed from the TS threshold determined above. Then the loads were computed from the above-derived stand mean DBH and tree height using Eqn 1 (QB2 hereafter).

Multiple comparisons (Chen *et al.* 1989) were conducted to determine if statistical differences existed between fuel load estimation errors from the aforementioned methods using the 70-fold cross-validation results.

Results

Fuel load estimations from stand characteristics

The statistics of stand characteristics, DBH and tree height, and loads of different fuel classes from the surveyed 70 plots are listed in Table 1. Basically, the variations of the stand characteristics are not very large compared with their mean values, but the standard deviations of each fuel load among all the plots are comparable with their mean values. However, the variation of the 10-h fuel is not as large as its mean value. This smaller load variation is reflected in the total dead fuel due to the larger contribution from the 10-h fuel.

As shown in Table 2, the regression relationships between field-measured stand characteristics and loads of each fuel are significant by the 70 cross-validations for litter, 1-h, 10-h, total dead fuel and total fuel. The coefficients of determination (R^2) exceed the significant level at 0.0001 for all fine fuels except 100-h and 1000-h fuels. Therefore, we excluded these two fuel classes from the SCB method analysis, which is presented below. The averaged RMSEs of fuel load estimations from stand characteristics of 70 validations are shown in the top row in Table 3. The errors increase as fuel lag-times increase. We discuss the remaining contents of Tables 2 and 3 when other estimation methods are discussed.

Fuel load estimations from the TM image

The regressed fuel load equations from TM1 are given in the middle of Table 2. The weak to moderate relationships between fuel loads and the one-pixel indices computed from the TM image suggest that the loads can barely be estimated by the SRB method. We will contrast this result with those from the TM2 method.

Table 2. Fuel load regression equations and their corresponding coefficients of determination (R^2) for each time-lag fuel load estimated by SC, TM1 and QB1

Independent predictive variables are stand characteristics of stand mean tree height (H), stand mean DBH (D), nth index from the compound TM indices, optimal shadow fractions computed for H and DBH (SF_{255} and SF_{212}), B_i, the value of band i, where i is the ith index computed from TM band values (25 indices used in total). Other variables are: L, fuel load; L_{td}, load of total dead fuel; L_{total}, load of total fuel. The asterisks for R^2: *, significant at 0.05 level; **, significant at 0.01 level; and ****, significant at <0.0001 level

Method	Estimation equations	R^2
SC	$L_{litter} = -2.188 + 0.372H - 0.128D$	0.57^{****}
	$L_{1\text{-h}} = -2.424 + 0.267H + 0.298D$	0.28^{****}
	$L_{10\text{-h}} = -1.392 + 0.295H + 0.314D$	0.29^{****}
	$L_{100\text{-h}} = -2.787 + 0.081H + 0.353D$	0.07
	$L_{1000\text{-h}} = -1.218 + 0.089H + 0.194D$	0.05
	$L_{td} = -1.001 + 1.106H + 1.031D$	0.42^{****}
	$L_{total} = -72.672 + 5.978H + 4.463D$	0.32^{****}
TM1	$L_{litter} = -4.275 + 29.268B_{16} + 1.543B_{18}$	0.156^{**}
	$L_{1\text{-h}} = 5.646 - 0.191B_{24}$	0.071^{**}
	$L_{10\text{-h}} = 7.23 - 0.173B_{24}$	0.055^{*}
	$L_{100\text{-h}} = -1.105 + 0.074B_{17}$	0.105^{**}
	$L_{1000\text{-h}} = 0.561 + 0.007B_1 - 23.626B_{16}$	0.124^{**}
	$L_{td} = 2.140 + 0.012B_3 + 3.783B_{19}$	0.173^{**}
	$L_{total} = 38.92 + 0.155B_{16} - 0.049B_{19}$	0.087^{*}
QB1	$L_{litter} = 0.002 + 5.284SF_{255} + 2.3675SF_{212}$	0.449^{****}
	$L_{1\text{-h}} = 2.209 + 16.923SF_{255} + 6.245SF_{212}$	0.270^{**}
	$L_{10\text{-h}} = 3.359 + 11.192SF_{255} + 1.090SF_{212}$	0.265^{**}
	$L_{100\text{-h}} = 2.513 - 9.987SF_{255} + 20.534SF_{212}$	0.033
	$L_{1000\text{-h}} = 1.197 - 0.310SF_{255} + 9.134SF_{212}$	0.0697
	$L_{td} = 9.281 + 13.102SF_{255} + 39.372SF_{212}$	0.354^{****}
	$L_{total} = 46.116 - 151.781SF_{255} + 465.875SF_{212}$	0.233^{**}

Stand mean DBH and tree height were determined from the TM indices, as shown in Table 4, with moderate R^2 and RMSEs at 1.47 cm and 2.23 m, when cross-validated. Although the RMSEs are much lower than the surveyed mean or median stand characteristics in Table 1, the magnitudes of the errors are still comparable with the surveyed standard deviation, indicating TM is having difficulty differentiating DBH and tree height from plot to plot. Although the significance analysis from the 70-plot cross-validation suggested that the correlations were not random, the small R^2 for TM in Table 4 indicates that fuel load

Table 3. Root mean square errors (Mg ha^{-1}) of fuel load cross-validation by all regression methods

Estimation errors in the same column with the same superscript indicate that they are not statistically different from each other at the 0.05 level. 100- and 1000-h fuel loads are not given owing to the weak relationship between stands characteristics and surveyed fuel loads

Method	Litter	1-h fuel	10-h fuel	100-h fuel	1000-h fuel	Total dead fuel	Total fuel
SC	0.686^{a}	1.831^{a}	1.946^{a}	–	–	5.022^{a}	32.860^{a}
TM1	1.006^{b}	2.215^{b}	2.535^{b}	2.801	2.286	6.957^{b}	38.998^{b}
TM2	0.962^{b}	2.108^{b}	2.281^{c}	–	–	6.452^{b}	37.111^{bc}
QB1	0.766^{cd}	1.822^{a}	1.958^{a}	–	–	5.383^{a}	34.570^{ac}
QB2	0.756^{ad}	1.805^{a}	1.943^{a}	–	–	5.317^{a}	34.483^{ac}

Table 4. Stand characteristics regression equations and their corresponding coefficients of determination (R^2) by compound indices from TM and by shadow fraction (SF) from QuickBird images

The subscripts of SF are the chosen threshold pixel values. All relationships are significant at: ****, <0.0001 level

Image	Equations	R^2
TM image	$D = 8.526 + 1.396B_{18} - 7.762B_{20}$	0.282****
	$H = 9.987 + 1.894B_{18} - 11.597B_{20} - 0.005B_{21}$	0.341****
QuickBird image	$D = 8.91 + 20.36\mathrm{SF}_{212}$	0.699****
	$H = 8.48 + 22.39\mathrm{SF}_{255}$	0.762****

estimations from these TM-deduced stand characteristics would be imperfect.

The load errors for all fuel classes estimated by either TM1 or TM2 are shown in Table 3. The errors from TM1 are significantly higher than those estimated from surveyed SC. Although these errors are reduced somewhat by TM2, it is not statistically better than TM1. Note that we should treat the errors by SC as the smallest errors TM2 could reach if stand characteristics were perfectly estimated. TM2 errors are still significantly higher than SC, with the largest for litter load, which is 40% more.

Fuel load estimations from QuickBird imagery

To estimate the fuel load from QuickBird (QB) imagery, we need to determine the TS threshold by optimising the coefficient of determination (R^2) with the threshold pixel value from the training data. Fig. 2 shows the R^2 of stand mean DBH and tree height with SFs computed at different TS thresholds of the QB panchromatic image. The optimal TS threshold for mean DBH is 212, with 0.699 for the maximum R^2 between mean DBH and shadow fraction. The optimal threshold for mean tree height is 255 with R^2 at 0.762. The regression equations of the two stand variables by SFs at these thresholds are listed in Table 4. These two regressed relationships correlate well with the training data. The RMSEs are 0.92 cm and 1.21 m for stand mean DBH and for stand mean tree height, and are considerably smaller than those from TM and the standard deviation from the survey.

Using these optimal SF_{212} and SF_{215}, the regressed fuel load equations from QB1 are given in the final part of Table 2. Similarly to SC, loads of litter, 1-h, 10-h and total dead fuels were better correlated with SF than those of 100-h and 1000-h fuels. The fine fuel estimates of QB1 are clearly superior to those of TM1. Applying SF values from the QB image on validating plots to the regressed equations of stand characteristics and SC

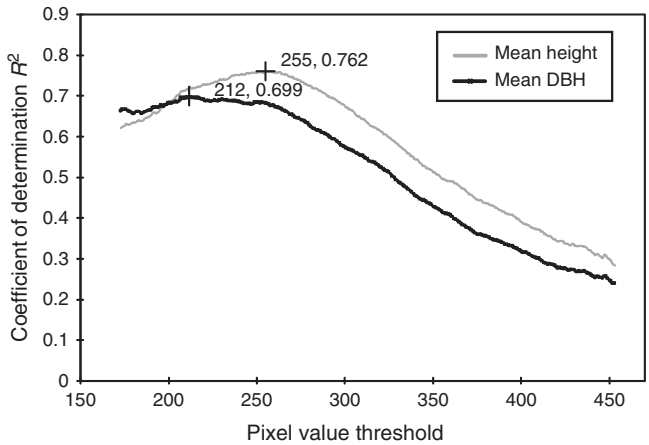

Fig. 2. Coefficients of determination between stand characteristics and shadow fractions as a function of pixel value thresholds in the panchromatic QuickBird image. The markers indicate optimal thresholds 212 and 255 with their corresponding coefficient of determination at 0.696 and 0.762, for mean diameter at breast height (DBH) and mean height.

in Tables 4 and 2 respectively, loads of all but coarse fuels can be estimated by method QB2.

The cross-validated RMSEs of QB1 and QB2 are confined to within 2.0 Mg ha^{-1} for each fine fuel, less than 6 Mg ha^{-1} for total dead fuel and less than 35 Mg ha^{-1} for total fuel, as shown in Table 3. However, for fuel classes with loads that can be estimated from the QB image, the results from these two methods are not significantly different. They are not even different from those of SC, except for litter by QB1. However, they are significantly different from the TM methods. The result of this multiple comparison suggests that the QB imagery

derivation is not comparable with the directly surveyed DBH and tree height in estimating fuel loads. Compared with the TM image, the RMSEs from QB were reduced by 27.2, 20.5, 18.2 and 17.6% for litter, 1-h, 10-h and total dead fuels. This shows that using the QB image improved the fine fuel load as well as the total dead fuel estimations quite substantially compared with those from the TM image. However, this improvement was not as evident with the increase of fuel size. When it comes to total fuel, using the QB image improved the fuel load estimation very little compared with TM.

Discussion and conclusion

To better estimate various types of fuel loads, regression methods using stand characteristics, TM and QB imagery were cross-validated against surveyed field results over 70 selected forest plots. As expected, loads of litter, 1-h fuel, 10-h fuel and total dead fuel were better estimated with smaller RMSEs using the VHRI QB image than using the TM image. However, using the QB image did not improve fuel load estimation for total fuel and showed very limited capability for estimating 100-h and 1000-h fuels.

One of the advantages of using VHRIs over TM images is texture analysis. Texture analysis on higher-resolution images such as QB can extract more information, so that the accuracy of the stand feature estimates can be improved. Kayitakire *et al.* (2006) showed similarly that stand structure variables could be well estimated from a texture analysis of an IKONOS-2 image. The errors of mean DBH and tree height estimates presented here are smaller than those in Kayitakire *et al.* (2006). We suspect this smaller error is due to the younger stands in our study area, which have smaller DBHs as well as tree height. It is consequently a relatively simple structure to resolve from the imagery.

Two factors contribute to the reason why QB1 outperformed TM1 and TM2. The first factor is the use of high-resolution multiband and panchromatic data, which made the SF method possible. Shadow fraction is usually associated with canopy closure, and thus highly correlated with mean DBH and tree height, especially for young to middle-aged stands. Thus the multipixel index from the QB image reflects better stand structure than the one-pixel TM index. Reinforced with the second factor that the fuel loads are closely associated with the stand characteristics, it is not surprising to see QB1 perform better than TM1 and even TM2 as the QB method takes individual stand characteristics into account. However, the unexpected result is that QB2 offers no advantage over QB1. In many cases, as with QB1, the QB2 regression yielded results approaching those of SC because their stand characteristics were accurately projected.

Our QB2 results indicate that the major sources of error were from the empirical relationships between stand characteristics and fuel loads. Apparently, there is still room for improvement, particularly for the relationship between coarse fuels and stand characteristics. The 100-h and 1000-h fuels were not closely related with the stand characteristics because these fuels are trees and branches felled mainly by strong wind. Thus, they possess very weak relationships with the stand characteristics and consequently reveal limited load estimation skill by either TM or QB images. As these types of fallen dead branches are primarily caused by strong wind, past history of meteorological conditions should be included as one of the regression parameters in future studies. Despite this limitation, QB imagery is still of great value in better estimating fine fuels. For fire management, fine fuel loads are critically important in rating fire danger and predicting surface fire behaviour.

Many stand characteristics are related to fuel load but are not accounted for in this study. Vegetation type is one such characteristic. Including vegetation type in the fuel loads regression is supposed to improve estimation, though this is not always the case (Skowronski *et al.* 2007). Determining vegetation classification from remote sensing data introduces additional errors. We have tried using vegetation-specific regressions to improve fuel load estimates from TM2 and QB2. The results showed only marginal improvement. This is because all our plots are secondary forest grown after several clear-cuttings and hence the heterogeneities among plots were not significant.

Another stand characteristic issue is the exclusion of stand age. In fact, stand age is one of the characteristics that affect the accumulation of fuels (Brandis and Jacobson 2003). To some extent it is even more important than mean DBH, tree height and canopy closure (Liu *et al.* 1995). Unfortunately, there is currently no method to obtain age information accurately from remote sensing data. All these factors potentially impair our ability to use satellite images for fuel load estimation and need further consideration.

Acknowledgements

The research was jointly supported by Forestry Public Interest grant number 200804002, NECT (New Century Excellent Talent) grant NCET-10–0278 from the China Ministry of Education, a Postdoctoral grant of Heilongjiang Province, and China National Nature Science Foundation grant number 30571508. This manuscript was co-prepared by a US government employee as part of his official duties, is not subject to copyright and is in the public domain. Opinions expressed in this publication may not necessarily reflect the position of the USDA. The use of trade names is for reader information and does not imply USDA endorsement of any product or service. We are indebted to the staff at the Yanjiang Forest Farm, Tahe Forest Bureau, Daxinganling Region, Heilongjiang Province, for their support in the fieldwork. We also extend our gratitude to Ms Diane Boomer for her thorough effort in improving the readability of the manuscript. We thank two anonymous reviewers for their very constructive comments and suggestions.

References

Andersen HE, McGaughey RJ, Reutebuch SE (2005) Estimating forest canopy fuel parameters using LIDAR data. *Remote Sensing of Environment* **94**, 441–449. doi:10.1016/J.RSE.2004.10.013

Arroyo LA, Healey SP, Cohen WB, Cocero D, Manzanera JA (2006) Using object-oriented classification and high-resolution imagery to map fuel types in a Mediterranean region. *Journal of Geophysical Research* **111**, G04S04. doi:10.1029/2005JG000120

Banninger C, Almer A, Ragam H, Wimmer A, Hogg J, Xanthopoulos G, Kalabokidis K, Coelho C, Ferreira A, Domingues C, Rodrigues J, Galante M, Rego F, Maia M (2002) FIREGUARD: mapping wildland fuels and infrastructure at the management unit level with very high spatial resolution satellite imagery for fire prevention and control in Mediterranean-type landscapes. In 'Forest Fire Research and Wildland Fire Safety'. (Ed. DX Viegas) pp. 113–126. (Millpress: Rotterdam)

Brandis K, Jacobson C (2003) Estimation of vegetative fuel loads using Landsat TM imagery in New South Wales, Australia. *International Journal of Wildland Fire* **12**, 185–194. doi:10.1071/WF03032

Brown JK, Oberheu RD, Johnson CM (1982) Handbook for inventorying surface fuels and biomass in the interior West. USDA Forest Service, Intermountain Forest and Range Research Station, General Technical Report INT-129. (Ogden, UT)

Chen HH, Ding ET, Cai XR, Hong W, Zhang ZY (1989) 'Statistics Applied in Forestry.' (Dalian Sea-transportation Press: Dalian) [in Chinese]

Deeming JE, Lancaster JW, Fosberg MA, Furman WR, Schroeder MJ (1972) The National Fire-Danger Rating System. USDA Forest Service, Rocky Mountain Forest and Range Experiment Station, Research Paper RM-84. (Fort Collins, CO)

Feng ZW, Wang XK, Wu G (1999) 'Biomass and Productivity of Forest Ecosystems in China.' (Science Press: Beijing) [in Chinese]

Giakoumakis MN, Gitas IZ, San-Miguel J (2002) Object-oriented classification modeling for fuel type mapping in the Mediterranean, using LANDSAT TM and IKONOS imagery – preliminary results. In 'Forest Fire Research and Wildland Fire Safety'. (Ed. DX Viegas) pp. 44–56 (Millpress: Rotterdam)

Hu HQ (2005) Predicting forest surface fuel load by using forest stand factors. *Scientia Silvae Sinicae* **41**, 96–100. [in Chinese]

Hu HQ, Wang Q (2005) Estimation of surface fuel load by stand factors. *Journal of Northeast Forest University* **33**(6), 17–18. [in Chinese]

Jia GJ, Burke IC, Goetz AFH, Kaufmann MR, Kindel BC (2006) Assessing spatial patterns of forest fuel using AVIRIS data. *Remote Sensing of Environment* **102**, 318–327. doi:10.1016/J.RSE.2006.02.025

Jin S (2002) Studies on fire regime of Heilongjiang province. III: Relationships between forest fires and forest types on a large scale. *Scientia Silvae Sinicae* **38**(4), 171–175. [in Chinese]

Kayitakire F, Hamel C, Defourny P (2006) Retrieving forest structure variables based on image texture analysis and IKONOS-2 imagery. *Remote Sensing of Environment* **102**, 390–401. doi:10.1016/J.RSE.2006.02.022

Keane RE, Mincemoyer AS, Schmidt KM, Long DG, Garner JL (2000) Mapping vegetation and fuels for fire management on the Gila National Forest Complex, New Mexico. USDA Forest Service, Intermountain Forest and Range Research Station, General Technical Report RMRS-GTR-46-CD. (Ogden, UT)

Keane RE, Burgan R, Van Wagtendonk J (2001) Mapping wildland fuels for fire management across multiple scales: integrating remote sensing, GIS, and biophysical modeling. *International Journal of Wildland Fire* **10**, 301–319. doi:10.1071/WF01028

Lasaponara R, Lanorte A (2007) On the capability of satellite VHR QuickBird data for fuel type characterization in fragmented landscape. *Ecological Modelling* **204**, 79–84. doi:10.1016/J.ECOLMODEL.2006.12.022

Leboeuf A, Beaudoin A, Fournier RA, Gundon L, Luther JE, Lambert MC (2007) A shadow fraction method for mapping biomass of northern boreal black spruce forests using QuickBird imagery. *Remote Sensing of Environment* **110**, 488–500. doi:10.1016/J.RSE.2006.05.025

Liu XD, Wang Z, Zhang DS, Sun YC, Weng GS, Zhao LQ (1995) Study on fuel model of larch stand in Daxinganling Region. *Forest Fire Prevention* **3**, 8–10. [in Chinese]

Miller JD, Danzer SR, Watts JM, Stone S, Yool SR (2003) Cluster analysis of structural stage classes to map wildland fuels in a Madrean ecosystem. *Journal of Environmental Management* **68**, 239–252. doi:10.1016/S0301-4797(03)00062-8

Mitri GH, Gitas IZ (2006) Fire type mapping using object-based classification of Ikonos imagery. *International Journal of Wildland Fire* **15**, 457–462. doi:10.1071/WF05085

Mitsopoulos ID, Dimitrakopoulos AP (2007) Allometric equations for crown fuel biomass of Aleppo pine (*Pinus halepensis* Mill.) in Greece. *International Journal of Wildland Fire* **16**, 642–647. doi:10.1071/WF06038

Mutlu M, Popescu SC, Stripling C, Spencer T (2008) Mapping surface fuel models using LIDAR and multispectral data fusion for fire behavior. *Remote Sensing of Environment* **112**, 274–285. doi:10.1016/J.RSE.2007.05.005

Olson JS (1963) Energy storage and the balance of producers and decomposers in ecological systems. *Ecology* **44**(2), 322–330. doi:10.2307/1932179

Oswald BP, Fancher JT, Kulhavy DL, Reeves HC (1999) Classifying fuels with aerial photography in east Texas. *International Journal of Wildland Fire* **9**, 109–113. doi:10.1071/WF00002

Reich RM, Lundquist JE, Bravo VA (2004) Spatial models for estimating fuel loads in the Black Hills, South Dakota, USA. *International Journal of Wildland Fire* **13**, 119–129. doi:10.1071/WF02049

Riaño D, Chuvieco E (2002) Generation of fuel type maps from Landsat-TM images and auxiliary data in Mediterranean ecosystem. PhD thesis, Alcalá de Henares University, Alcaláde Henares, Spain.

Scott K, Oswald B, Farrish K, Unger D (2002) Fuel loading prediction models developed from aerial photographs of the Sangre de Cristo and Jemez mountains of New Mexico, USA. *International Journal of Wildland Fire* **11**, 85–90. doi:10.1071/WF01044

Shan YL, Zhang M, Hu HQ (2005) Models for surface fuels of *Pinus sylvestris* var. *mongolica* forests in Daxing'anling region. *Journal of Northeast Forest University* **33**(2), 74–75. [in Chinese]

Sikkink PG, Keane RE (2008) A comparison of five sampling techniques to estimate surface fuel loading in montane forests. *International Journal of Wildland Fire* **17**, 363–379. doi:10.1071/WF07003

Skowronski N, Clark K, Nelson R, Hom J, Patterson M (2007) Remotely sensed measurements of forest structure and fuel loads in the Pinelands of New Jersey. *Remote Sensing of Environment* **108**, 123–129. doi:10.1016/J.RSE.2006.09.032

Wang Q, Jin S (2008) Estimation of forest fuel load in Maoershan Forest using remote sensing image and stand factors. *Journal of Northeast Forestry University* **136**(6), 34–36. [in Chinese]

Zhang YP (2008) Study on the impacts of climate change on forest fires in Daxing'anling Mountains. MSc Dissertation, Northeast Forestry University, Harbin, Heilongjiang Province, China. [in Chinese]

Zhang XC, Huang ZC, Zhao HY (2003) 'Processing of Digital Remote Sensing Images.' (Zhejiang University Press: Hangzhou) [in Chinese]

Zhao XW (2001) Important advancement in remote sensing of forest resources. *China Engineering* **3**(8), 15–25. [in Chinese]

Zhao XW, Li CG (2001) 'Quantitative Estimation of Forest Resources Based on 3S Technology.' (Chinese Science and Technology Press: Beijing) [in Chinese]

Zhou YL (1991) 'Vegetation in Daxing'anling Mountains.' (Science Press: Beijing) [in Chinese]